Discovery Immunology, 2024, **3**, kyae007
https://doi.org/10.1093/discim/kyae007
Advance access publication 25 May 2024
Research Article

Research Article

Lunar-linked biological rhythms in the immune system of freshwater three-spined stickleback

Joseph A. Jackson[1,*], Alexander Stewart[2] and Joanne Cable[3]

[1]School of Science, Engineering and Environment, University of Salford, Salford, UK
[2]Faculty of Health and Medical Sciences, University of Surrey, Guildford, UK
[3]School of Biosciences, Cardiff University, Cardiff, UK

[*]Correspondence: Joseph A. Jackson, School of Science, Engineering and Environment, University of Salford, Salford M5 4WT, UK. Email: j.a.jackson@salford.ac.uk

Abstract

Immune responses are widely accepted to be under circadian regulation via a molecular clock, with many practical consequences, but much less is known of how other biological rhythms could affect the immune system. In this study, we search for lunar rhythms (circalunar, circasemilunar, and circatidal cycles) in the immune expression of the recently marine-derived freshwater fish, the low-plate morph of the three-spined stickleback. We employed time series of immune expression (mRNA) measurements for 14 immune-associated genes, representing a variety of immunological pathways. Times series measurements were taken on fish populations in the wild, in seminatural outdoor mesocosms, and in the laboratory, according to sampling regimens originally designed to study circannual variation but with the additional potential to provide information about lunar variation. Our evidence best supported the existence of a very small endogenous tidal rhythm. This is consistent with previous suggestions of the existence of a primordial tidal endogenous clock, some elements of which may be conserved in animals evolving outside the marine environment.

Graphical Abstract

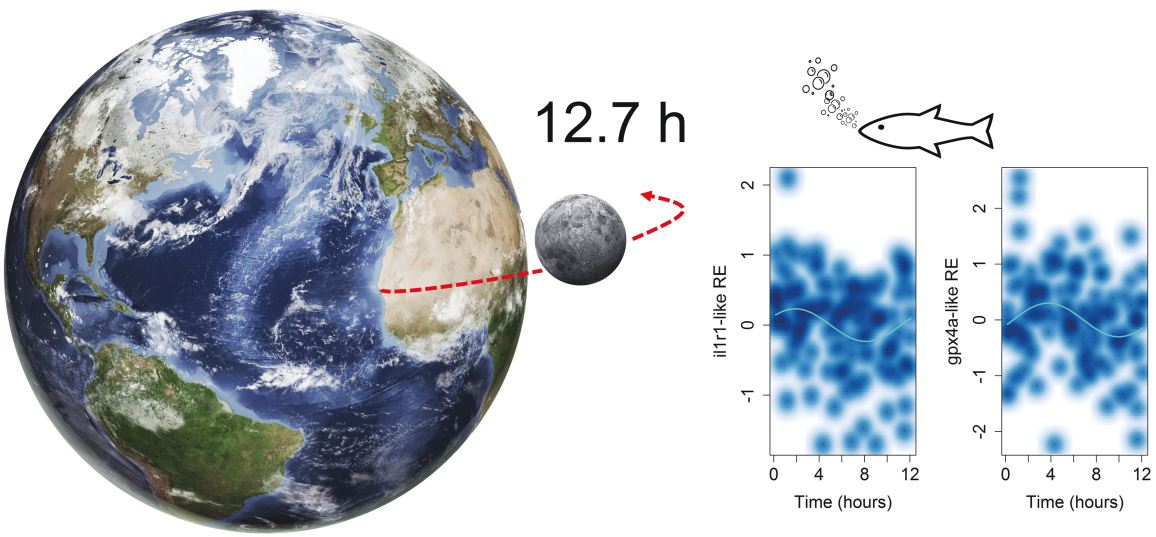

Keywords: immunity, tidal, ultradian, lunar, three-spined stickleback

Abbreviations: LMM: linear mixed model; MLMM: multivariate linear mixed model; QPCR: quantitative reverse transcription PCR; UTC: Coordinated Universal Time; VIF: variance inflation factor.

Introduction

The vertebrate immune system is widely understood to be influenced by a circadian (24-hour) clock [1], but whether other, non-circadian cycles have a role in determining immune expression is less studied. Biological rhythms linked to the relative astronomical position of the moon are important for

Received 30 December 2023; Revised 7 April 2024; Accepted for publication 3 June 2024

life processes in marine organisms [2–4] and have recently been proposed as the evolutionary precursor for an ultradian 12-hour dawn–dusk transcriptional rhythm in mice that involves many immunological transcripts [5–7]. This murine dawn–dusk rhythm may be controlled by an independent molecular clock [5] to the well-known circadian clock [8, 9] that regulates immunity in mice. In the present study, we test for the importance of lunar rhythms in the immune expression of a recently marine-derived peri-coastal vertebrate, the freshwater low-plate morph [10] of the three-spined stickleback (*Gasterosteus aculeatus*). We reasoned that, outside of the immediate marine environment, such an organism should be amongst the most likely to show the effects of primordial lunar cycles if a molecular clock machinery for these exists and can be conserved in non-marine settings.

In *G. aculeatus*, a pronounced circannual oscillation in immune gene expression has previously been demonstrated in the natural populations we study here [11], although this is driven by thermal and dietary variation and not by a molecular clock or photoperiodic cues. In the present study, we will focus on the possibility of further modalities, linked to the position of the moon, which could have biological relevance under the conditions experienced by peri-coastal *G. aculeatus*. For this, we employ long-term gene expression datasets that we have previously generated for the purpose of studying circannual variation. These datasets are based on approximately calender-monthly sampling of fish in natural sites and mesocosms over 2 years, and weekly sampling of fish in an experimental laboratory population subject to controlled photoperiod and homogenous conditions over 31 weeks [11, 12]. The modalities we search for are those associated with the position of the moon and that drive important environmental cycles. These are circatidal oscillation, varying with the approximately twice-daily ebb and flow of the tides; circasemilunar oscillation, varying with the approximately two-weekly neap-spring cycle of tidal amplitude; and circalunar oscillation, varying with the new moon–full moon phase cycle that approximates to a synodic month. The sampling points for our datasets were executed around 12:00 UTC, placing them in the middle of the day at our study latitude and thus approximately centring out the effect of any constant circadian rhythm or harmonics thereof. Importantly, the fact that the sampling intervals (calendar monthly in the field and mesocosms and weekly in the lab experiment) are never exact higher harmonics of the modalities of interest means that their phase point shifts at every sampling point, allowing statistical evaluation.

There are several reasons to consider the possible importance of lunar cycles in freshwater *G. aculeatus*. This is an ancestrally marine species in which some populations (such as those in the British Isles) invaded freshwater habitats as these became available as the last ice age receded, approximately 10 000–20 000 years ago [13]. Moreover, some populations of freshwater *G. aculeatus* (including one of the populations studied here) still occur in or close to zones of marine influence [14]. In such zones, changes in the height of the water column and in current strength, or in associated physicochemical parameters, varying with circatidal and circasemilunar oscillation, could affect organismal behavior and the physiology and behavior of predators and prey. Circalunar cycles could also be directly relevant for both freshwater and marine organisms in shallow waters as they affect illumination at night, which, in turn, affects foraging and predation risk [15].

In summary, in this study, we used long-term field and experimental datasets on immunological gene expression in wild peri-coastal three-spined sticklebacks of the low-plate morph to search for the presence of lunar expression cycles. We robustly detected a small amplitude tidal cycle in laboratory stickleback populations (the latter isolated from any environmental tidal influence). This is consistent with the presence of an endogenous circatidal clock that has effects on the immune system and that can be conserved outside of the immediate marine environment.

Methods and Materials

Data

We use the datasets described in detail in Ref. [11], which are based on two separate studies of freshwater low-plate morph three-spined sticklebacks in coastal areas of Wales. The first of these studies was of freshwater field sites, exposed to natural lighting and weather, in the Aberystwyth area of Mid Wales. These sites included a side channel of a lowland river (52.4052, –4.0372), an upland lake (52.3599, –3.8776), and an array of outdoors mesocosms (52.4151, –4.0670) stocked from the lake (described in detail in Ref. [12]). The river site was non-tidal and situated c. 3.5 km from the sea at an elevation of c. 10 m; the lake was situated c. 14 km from the sea at an elevation of c. 280 m. The sites were sampled approximately calendar monthly across two annual cycles between October 2013 and December 2015. For gene expression measurements, 5 fish per month each were sampled from both the river and lake and 10 fish per month from the mesocosms. In the case of the mesocosms (whose implementation is described in detail in Ref. [12]), these were initially stocked with acclimated, parasite-treated post-larval fish from the lake in late summer 2013 and these fish were studied from October 2013 until September 2014. The mesocosms were then refitted [11, 12] and restocked with a further cohort of acclimated parasite-treated post-larval fish from the lake, which were studied from December 2014 until November 2015. Datasets of, respectively, 217, 235, and 446 fish for the river, lake, and mesocosms were ultimately assembled with no missing values for the variables analyzed below. The second (experimental) study was of a population of laboratory fish originally captured in Roath Brook, Cardiff, South Wales (a non-tidal freshwater habitat c. 3 km from the sea at an elevation of c. 10 m; 51.499858°, –3.168780°), and acclimatized to laboratory conditions, including anti-parasitic treatment. Fish were maintained in aquaria in a factorial design with two photoperiodic regimens and two constant temperature treatments and otherwise homogenous conditions. Four fish per week were sampled for gene expression measurements for 31 weeks giving a dataset of 124 fish with no missing values for the variables analyzed below. The experiment and maintenance conditions are described in detail in Ref. [11]. Sampling points in both the field and laboratory studies were around the middle of the day (12:00 UTC), tending to negate the effect of any constant circadian rhythm. For both studies a standard set of 14 expression measurements [16] were taken in whole-fish mRNA pools for the genes *defbl2* (ENSGACG00000020700; a beta defensin antimicrobial peptide [17]), *cd8a* (ENSGACG00000008945; the T-cell receptor

co-receptor alpha chain from cytotoxic T-cells [18]), *foxp3b* (ENSGACG00000012777; the regulatory T-cell transcription factor forkhead box P3 [19]),*gpx4a* (ENSGACG00000013272; the anti-oxidative enzyme, glutathione peroxidise 4a [20]), *ighm* (ENSGACG00000012799; the heavy chain of immunoglobulin M [21]), *ighz* (the heavy chain of immunoglobulin Z, see [22]), *il12ba* (ENSGACG00000018453; a subunit of the pro-inflammatory T-helper cell type 1 cytokine interleukin 12 [23]), *il17d* (ENSGACG00000001921; a cytokine of the pro-inflammatory interleukin 17 family [24]), *il1r1*-like (ENSGACG00000001328; Interleukin 1 receptor type 1-like involved in interleukin 1 family signaling [25]), *il4* (a piscine homolog of the mammalian T-helper cell type 2 cytokine interleukin 4 and interleukin 13 lineage, see [26, 27]), *lyz* (ENSGACG00000018290; the bacteriolytic enzyme lysozyme [28]), *orai1a* (ENSGACG00000011865; a calcium channel known to be necessary for T-cell activation and proliferation in mammals [29]); *tbk1* (ENSGACG00000000607; TANK-binding kinase 1, involved in innate inflammatory signaling [30]), and *tirap* (ENSGACG00000006557, Toll/Interleukin-1 Receptor Domain-Containing Adapter Protein, involved in innate inflammatory signaling [31]). As described in detail in Ref. [16], levels of mRNA were measured via two-step quantitative reverse-transcription PCR (QPCR) and expressed as relative expression values indexed to a calibrator sample employing the $2^{-\Delta\Delta CT}$ algorithm [32]. Normalization was carried out to two endogenous control genes *acvr1l* (ENSGACG00000010017; Activin A receptor type 1 like) and *yipf4* (ENSGACG00000002189; Yip1 domain family, member 4). These endogenous control genes have previously been validated to show stable seasonal expression as a pairing (where the normalization is to the geometric mean of the two control genes) [33]. They did not show any lunar periodicity in their raw threshold cycle values when these were analyzed by confounder-adjusted cosinor regression (as below). Taken together the gene expression data reflect a wide variety of immune response pathways, and, in the case of *gpx4a*, antioxidant function that correlates positively with high immune activity [16]. Also included in the data set are host length, sex, reproductive state, the date of sampling, and in the case of the laboratory experiment, the treatment level for temperature treatment (7°C or 15°C). The photoperiod treatment levels for the laboratory experiment are not included in the analyses here as they had no significant effect [11]. Physical data relating to different cycles were obtained as follows. Day length on given sampling dates was calculated using the *daylength* function [34] in the *geosphere* package of *R* [35]. Moon phase data (% of the lunar disc illuminated) were obtained from the web pages of the Astronomical Applications Department of the US Naval Observatory [36]. Tidal amplitudes and tidal heights are based on data published by the UK Hydrographic Office for Aberystwyth in the case of the mid-Wales sites and for Cardiff in the case of the south Wales sites.

The animal studies generating the datasets employed in the present study have, as noted above, previously been thoroughly described [11, 12, 16] and fully followed institutional and national ethical regulations and guidelines, as previously documented [11, 12, 16]. Work involving regulated scientific procedures as defined in the Animal (Scientific Procedures) Act 1987 (ASPA) was conducted under UK Home Office (HO) License PPL 302876 held at Cardiff University and all other work was designed in consultation with the ASPA HO inspectorate.

Physical background and collinearity between cycles

We have previously studied circannual cycles in the immune expression of low-plate-morph freshwater three-spined sticklebacks from coastal areas of Wales, finding a very large environmentally driven modality in wild sticklebacks and a small endogenous modality, with distinct gene involvements and phase relationships to the wild modality, in animals maintained under homogenous laboratory conditions [11]. Here, bearing in mind the context of circannual variation, we additionally consider the possibility of lunar rhythmicity in immune expression in the same populations of sticklebacks. We note that our previous studies establish that environmental temperature and diet variation are necessary and sufficient to explain the major circannual immunophenotypic variation seen in wild sticklebacks and exclude a role for an endogenous clock in driving this major modality [11, 37] and that this exclusion would logically extend to lunar endogenous clocks.

Each of the cycles that we consider here can be represented by a physical quantity that is linked to the ultimate physical environmental drivers of biotic effects (such as lighting in the case of annual and lunar cycles and current strength in the case of semilunar and tidal cycles). This quantity is day length in the case of circannual cycles, proportion of the lunar disc illuminated in the case of lunar cycles, tidal amplitude in the case of semicircalunar cycles, and tidal height in the case of tidal cycles. Nonetheless, any biological rhythm with a period corresponding to one of these cycles might be out of phase with the physical drivers and thus not necessarily temporally correlated with them. For example, this might be due to time lags as effects cascade through environmental and organismal interaction networks. In order to detect cycles with a given period, but with unknown acrophase (peak/trough timing) and amplitude, we employ cosinor regression [38, 39], which was originally developed to identify cycles with predefined periods in relatively short and sparse time series. Importantly for the field-based study, which was designed to study circannual variation, the monthly sampling regimen employed led to significant collinearity amongst some of the annual and lunar physical variables and the cosinor regression terms used to describe them (see Figs 1 and 2). For the field-based study, we thus proceeded with an analysis on the basis that this might be somewhat informative, but any results would require careful qualification in the light of the known collinearity. As the circannual cycle was dominant, for analysis of the lunar rhythms in the field study we (conservatively) analyzed residuals from base models describing circannual variation and confounder variables, asking whether lunar cycles could account for any variation over and above the known circannual cycle. In the case of the laboratory study, which had a weekly sampling regimen, collinearity amongst cyclical physical variables and cosinor terms was more limited (see Figs 3 and 4) and analysis of all cycles could thus be carried out within a single model and results interpreted more straightforwardly.

Analyses

All analyses were conducted in *R* version 4.3.1 [40]. Gene expression data tended to have distributions with right-hand skews and so prior to analysis we evaluated different normalizing data transformations using the *bestNormalize*

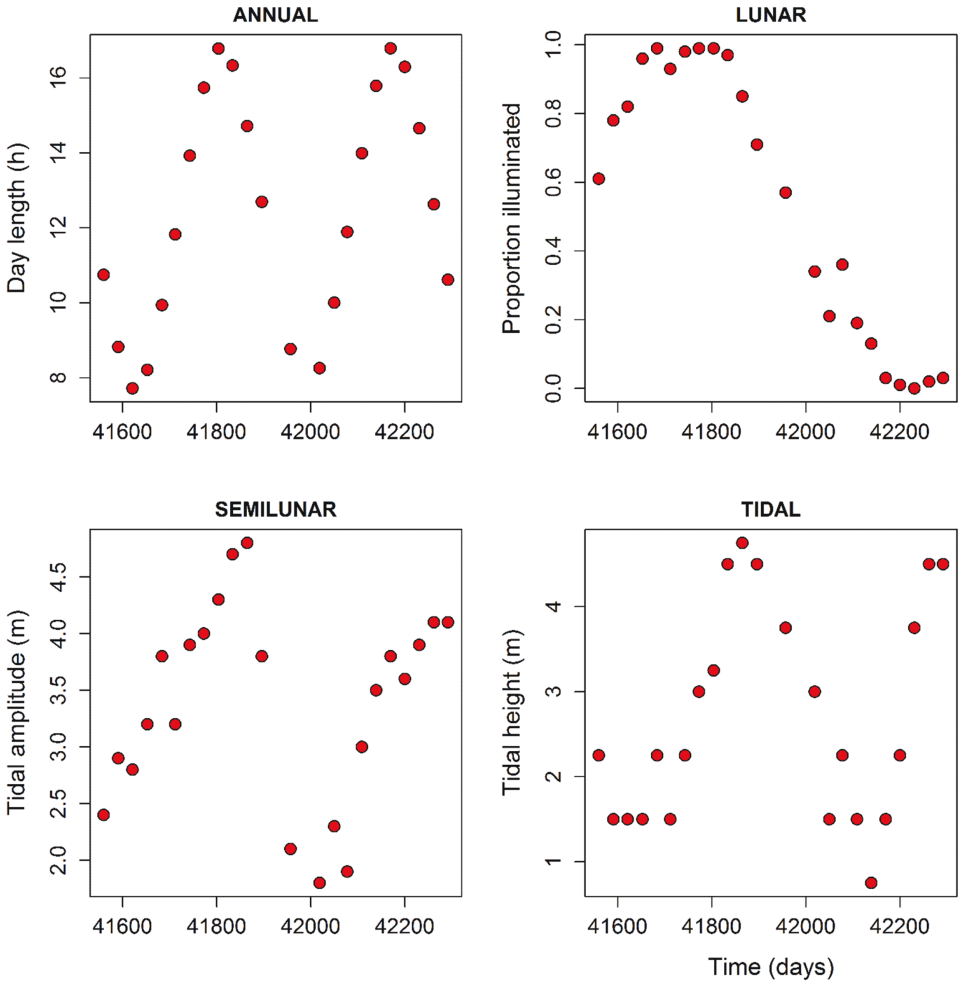

Figure 1: scatterplots of the physical quantities representing the different cycles considered in this study against time (epoch 00:00 h 1 January 1900); points represent individual sampling occasions in the field sampling regimen (river, lake, and mesocosms). Annual variation is represented by photoperiod; lunar variation is represented by the proportion of the lunar disc illuminated; semilunar variation is represented by tidal amplitude on the adjacent coastline; and tidal variation is represented by tidal height on the adjacent coastline

package [41]. For consistency, we applied an ordered quantile normalization transformation (*orderNorm* function) to all gene expression variables, as this was most frequently the optimal transformation and gave good results in all cases. Data were analyzed separately for each field site (river, lake, and mesocosms) and for the laboratory study. To provide high-level, overall hypothesis tests of the existence of lunar cycles in gene expression data, avoiding excessive multiple testing, we employed multivariate linear mixed models (MLMMs) with all 14 gene expression variables as responses at each site for each cycle. For the gene expression variables at the field sites, as noted above, we have previously demonstrated a large circannual oscillation in gene expression driven by thermal variation and diet. Thus, for these sites, for each gene, prior to the MLMM analysis, we constructed a base linear mixed model (LMM) with fixed terms that accounted for circannual oscillation (continuous cosinor variables), host length (continuous), sex (factor), reproductive state (factor), infection with the larval tapeworm *Schistocephalus* (factor), and year (factor). We additionally included interactions between the circannual cosinor terms and year to allow for the differences in seasonality between years that we have previously observed. A random term was employed in the LMM to represent technical variation between assay plates (see Ref. [11]). To assess the presence of lunar cycles in site-specific MLMMs, we then separately fitted a cosinor model with each of the lunar periods to the 14 sets of residuals from the circannual base LMMs, asking whether the lunar cycles could explain any variation additional to that explained by circannual variation. MLMMs were implemented with the *MCMCglmm* function in the *MCMCglmm* package [42] and additionally contained a random term for assay plate. The significance of cosinor terms for the respective biological rhythms of interest was assessed by a Wald test using the posterior means and posterior covariances. These high-level tests were carried out first for the field sites, arbitrarily setting the periods at 12.4 hours, 14 days, and 28 days, respectively, for the tidal, semicircalunar, and circalunar cycles. As described further below, in these tests, there was a highly significant effect for the circasemilunar cycle but not for other lunar cycles at the field sites. We then secondarily, for each cycle, assessed values of the period 10 increments (of c. 7% cycle length) either side of widely quoted precise astronomical estimates (12.4 hours, tidal; 14.7 days, semicircalunar; and 29.5 days, circalunar). This confirmed the significance of the semicircalunar cycles (that were most significant at a period

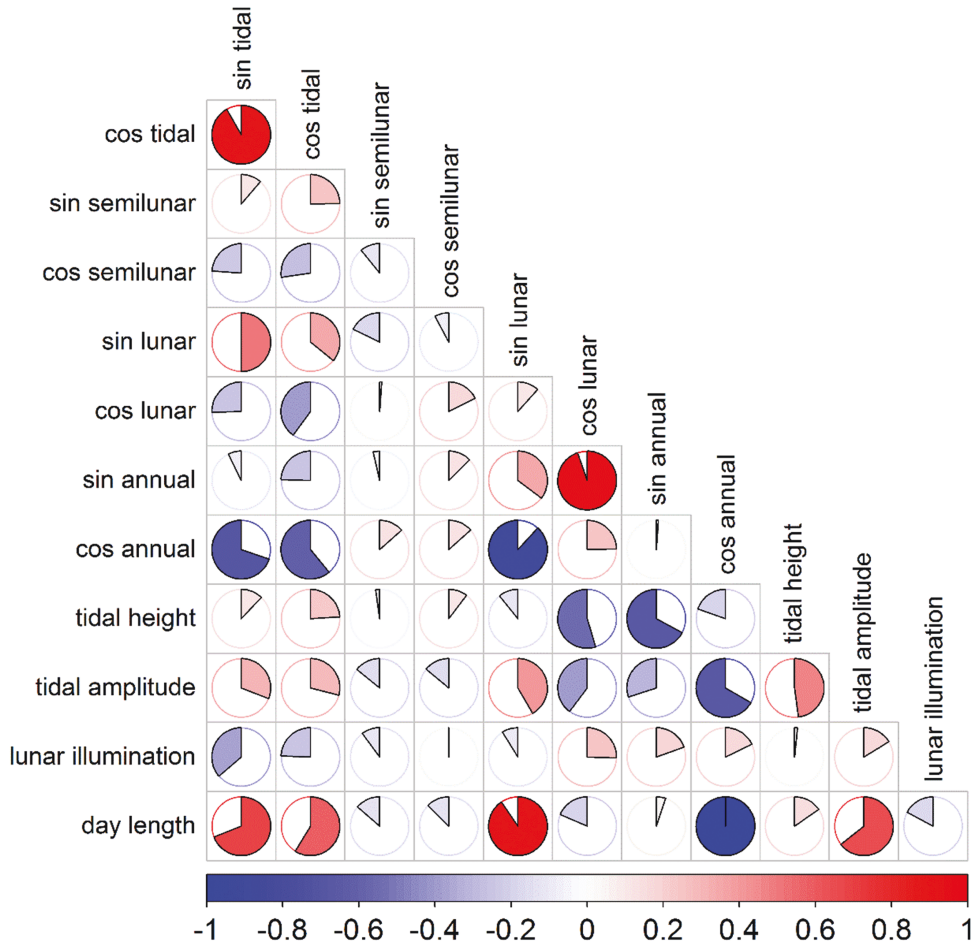

Figure 2: matrix pie chart plots for the field sampling regimen (river, lake, and mesocosms) showing Pearson correlations between the cosinor terms used to represent different cycles in overall analyses and also the physical quantity for each cycle (annual variation = photoperiod; lunar variation = proportion of the lunar disc illuminated; semilunar variation = tidal amplitude on the adjacent coastline; tidal variation = tidal height on the adjacent coastline). Clockwise-orientated segments represent positive correlations

of 13.9–14 days) and lack of significance for other cycles. We then employed the original period settings of 12.4 hours, 14 days, and 28 days in subsequent analyses (as these offered no disadvantage over any other settings investigated), beginning with high-level MLMM tests for the lunar cycles in the laboratory fish, and then continuing with post hoc testing of individual gene expression variables for all sites and cycles (see below). MLMM analyses of the laboratory fish were on the unmodified transformed gene expression variables due to the smaller circannual cycle in this setting and much-reduced collinearity between the cyclical explanatory variables (see above). In these cases, each MLMM contained the 14 gene expression variables as responses. The fixed explanatory terms included cosinor terms for circannual, circatidal, circasemilunar, and circalunar cycles, and host length (continuous), sex (factor), and reproductive state (factor). An additional fixed factor was included to account for the effects of a 7°C versus 15°C thermal manipulation [11] applied during the experiment (which were substantial) but terms representing photoperiodic regimen [11] were not included as this was not previously found to be significant [11]. A random term was employed to represent technical variation between assay plates.

In order to further characterize the effects found in overall multivariate MLMM tests, we carried out post hoc LMM analysis of individual gene expression variables for all cycles at all sites. In the case of LMMs for the field sites, we analyzed the same residuals from base circannual LMMs as the response, and the same explanatory variables, as employed in the MLMMs for these sites (see above). For the post hoc LMM analysis of individual gene expression variables in the laboratory experiment, we used the transformed gene expression variables as the response and the same explanatory variables as in the corresponding MLMMs. In all LMMs, the significance of cosinor terms in each gene vs lunar cycle combination was assessed by a 2-degree-of-freedom likelihood ratio deletion test from a full model. All LMMs were implemented in the *lme4* package [43] using the *lmer* function.

In addition to the overall MLMM tests, for each habitat or experiment, we also combined the LMM cosinor terms deletion test *P* values for each lunar cycle across all 14 genes by the Fisher method [44]; this produced a pattern of overall significance consonant with that found via the MLMM analysis. For gene expression variables within habitats or experiments that showed individual significance for a given cycle, where this cycle was also significant overall across all gene expression variables, we calculated the cycle acrophase from the estimated LMM coefficients for the cosinor terms [38, 45]. We compared this acrophase to the acrophase for a cycle of

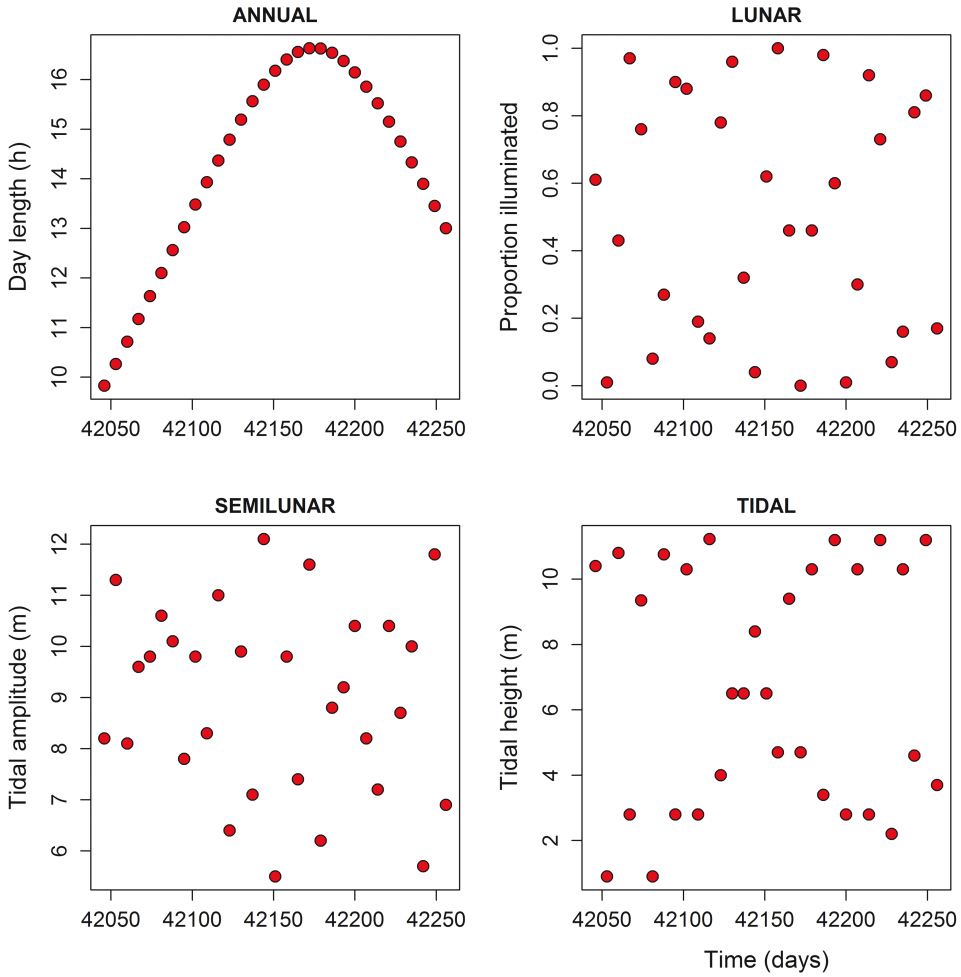

Figure 3: scatterplots of the physical quantities representing the different cycles considered in this study against time (epoch 00:00 h 1 January 1900); points represent individual sampling occasions in the laboratory sampling regimen. Annual variation is represented by photoperiod; lunar variation is represented by the proportion of the lunar disc illuminated; semilunar variation is represented by tidal amplitude on the adjacent coastline; tidal variation is represented by tidal height on the adjacent coastline

the same period fitted to the corresponding physical variable at the nearby coast.

For all of the above analyses, collinearity involving cosinor explanatory terms and also the physical variables associated with each cycle was evaluated by (Pearson) correlation analysis (see Figs 2 and 4). We calculated Variance Inflation Factors (VIFs) for the cosinor terms within given model structures employing the *vif* function in the *car* package. We considered a VIF > 10 to represent high collinearity. In order to quantify the total amount of variation explained by cosinor terms in LMMs we used the *calcVarPart* function in the *VariancePartition* package [46]. $P = 0.05$ is taken as the significance cutoff. For the higher level, overall multivariate (MLMM) tests of the lunar cycles, if a Bonferroni multiplicity adjustment is applied separately to the field and experimental studies (which were independent) then all of the reported significant P values are significant at the $P = 0.05$ level.

Results

Lunar cycles in natural habitats and semi-natural mesocosms

Consonant with previous analyses based on the same dataset, our present analysis reflected a very dominant circannual expression cycle in wild fish that was diminished but still prominent in mesocosm fish (see Fig. 5). Importantly, given the monthly sampling regimen over 2 years, there was collinearity (Figs 1 and 2) amongst some of the cosinor functions for the circannual cycle and the different lunar cycles and their associated physical quantities. In full cosinor models containing sinusoidal terms for all of the cycles considered, VIF was high for circalunar terms (c. 15–25 at the initial period settings employed) and circatidal terms (c. 10–15) although lower for circasemilunar terms (c. 1–2). Given this pattern of collinearity we (conservatively) searched for circatidal, circasemilunar, and circalunar cycles in the residuals from base models for circannual variation, asking whether such cycles could explain any additional variation. This analysis provided consistent statistical evidence for apparent circasemilunar-like cycles occurring at all three sites, which was most detectable at a period of 13.9–14 days. In the case of a 14-day period, there was overall significance, in each case, for the upland lake (MLMM, $X^2 = 63.6$, $DF = 28$, $P = 1.4 \times 10^{-4}$), the lowland river ($X^2 = 55.0$, $DF = 28$, $P = 1.7 \times 10^{-3}$), and the outdoor mesocosms ($X^2 = 105.7$, $DF = 28$, $P = 5.9 \times 10^{-11}$). Significance for individual genes (at a 14-day period) occurred for *il4* in all three habitats, for *tirap* in the river and mesocosms, for *lyz* in the lake and mesocosms, for *il17*

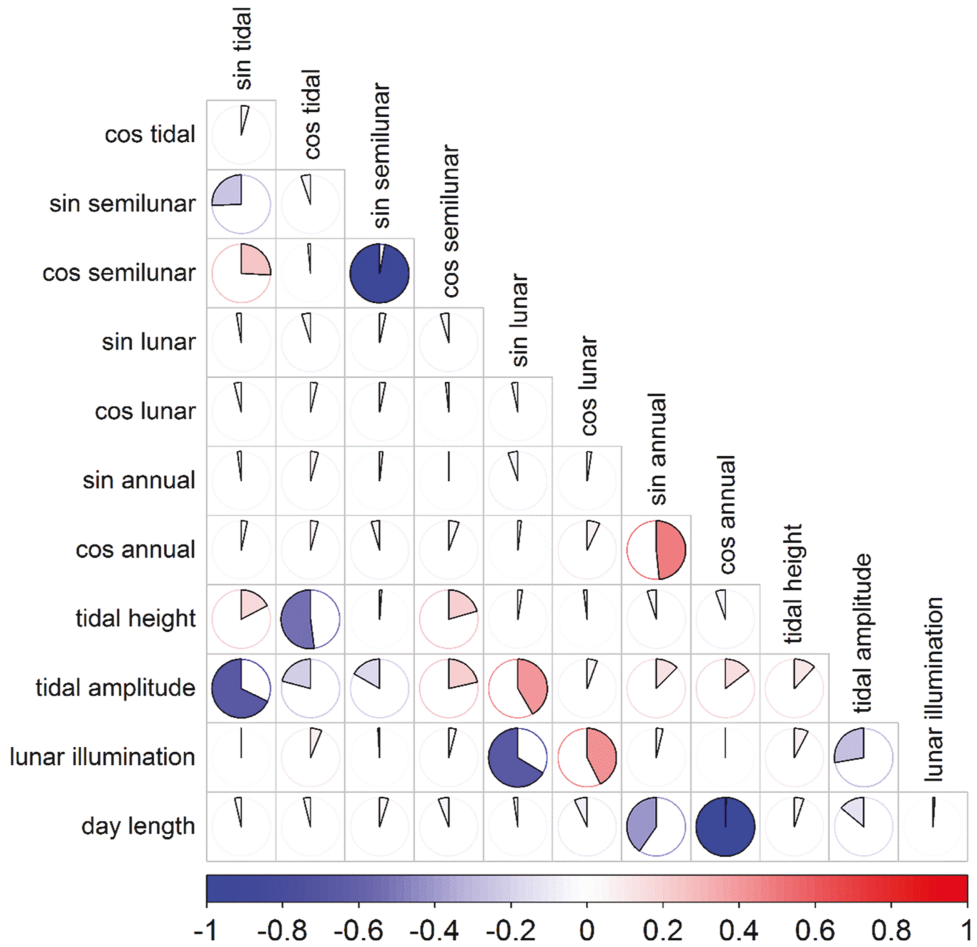

Figure 4: matrix pie chart plots for the laboratory sampling regimen, showing Pearson correlations between the cosinor terms used to represent different cycles in overall analyses and also the physical quantity for each cycle (annual variation = photoperiod; lunar variation = proportion of the lunar disc illuminated; semilunar variation = tidal amplitude on the adjacent coastline; tidal variation = tidal height on the adjacent coastline). Clockwise-orientated segments represent positive correlations

in the lake, and for *bdef*, *ighm*, and *il1rl* in the mesocosms (Fig. 5). The expression acrophases in significant genes indicated expression maxima in the high amplitude half of the circasemilunar cycle for *lyz*, *il1rl*, *gpx4a*, and *defb*, and expression maxima in the low amplitude half of the cycle for *il4*, *tirap*, *ighm*, and *il17* (Fig. 6). Given the collinearity amongst the different cycles studied, however, the possible origin of these apparent circasemilunar cycles through correlation with other cycles should be borne in mind (considered further in Discussion). There was no overall significance for circatidal cycles at any of the sites, although there were significant individual gene results for *orai1* in the river, *cd8* in the lake, and *ighm*, *lyz*, and *tirap* in the mesocosms at a 12.4-hour period. There was no evidence of circalunar cycles.

Lunar cycles under homogenous laboratory conditions

Collinearity amongst circannual and lunar model terms was limited in the weekly laboratory sampling regimen (Figs 3 and 4) (VIF for terms in full model < 2, excluding one or other of the semilunar sinusoid terms, which were correlated). There was overall support for a small circannual oscillation in laboratory fish (as previously reported) (Fig. 5), with different timing to the major circannual cycle seen in wild fish. The effects of this were detectable in 5/13 individual genes (*cd8*, *ighz*, *il4*, *orai1*, and *tbk1*), accounting for only a limited amount of the total variation (4–11%) in these cases. There was also overall support ($X^2 = 52.45$, $DF = 28$, $P = 3.4 \times 10^{-3}$) for a very small tidal oscillation that was detectable individually in 2/13 genes (*gpx4* and *il1rl*) (see Table 1) at a 12.4-hour period but with a further six genes (*bdef*, *cd8*, *foxp3*, *il17*, *tbk1*, and *tirap*) with $P < 0.2$. Variation explained was <2% for both of the individually significant genes. The predicted acrophases for these indicated maximum expression around high tide on the adjacent coast (Figs 6 and 7). There was no overall support for the existence of circasemilunar or circalunar oscillation, although two genes (*bdef* and *foxp3*) showed individually significant results for circasemilunar oscillation (at a 14-day period).

Discussion

We found evidence for a small endogenous tidal oscillation in the immune system of peri-coastal 3-spined sticklebacks from the western coast of Britain. Analyzing 14 immune-associated genes, we robustly detected an overall circatidal cycle of mRNA expression in laboratory-maintained animals. Circatidal cycling was detectable for two individual genes.

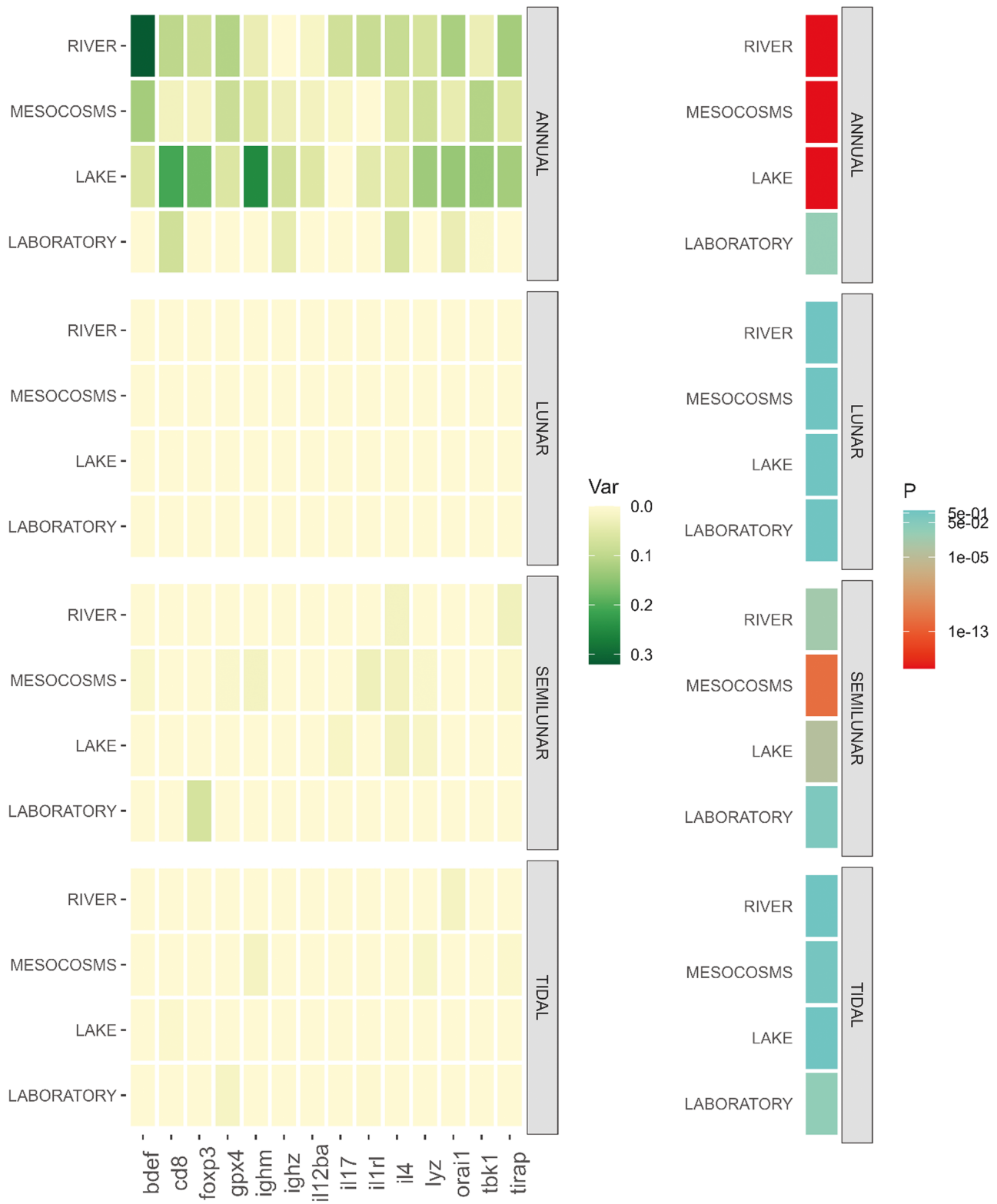

Figure 5: heat maps indicate the percentage of variation in the expression of individual genes explained by different cycles (left panel) and the overall significance (across all genes) of the cycles (right panel) for the river, lake, mesocosm, and laboratory populations. Var, % of total variance explained in each gene in a LMM; *P*, overall *P* value for the cosinor terms in an MLMM. In the case of the lunar cycles for the field sites, the % total variance explained is scaled by the residual variation from the circannual base model

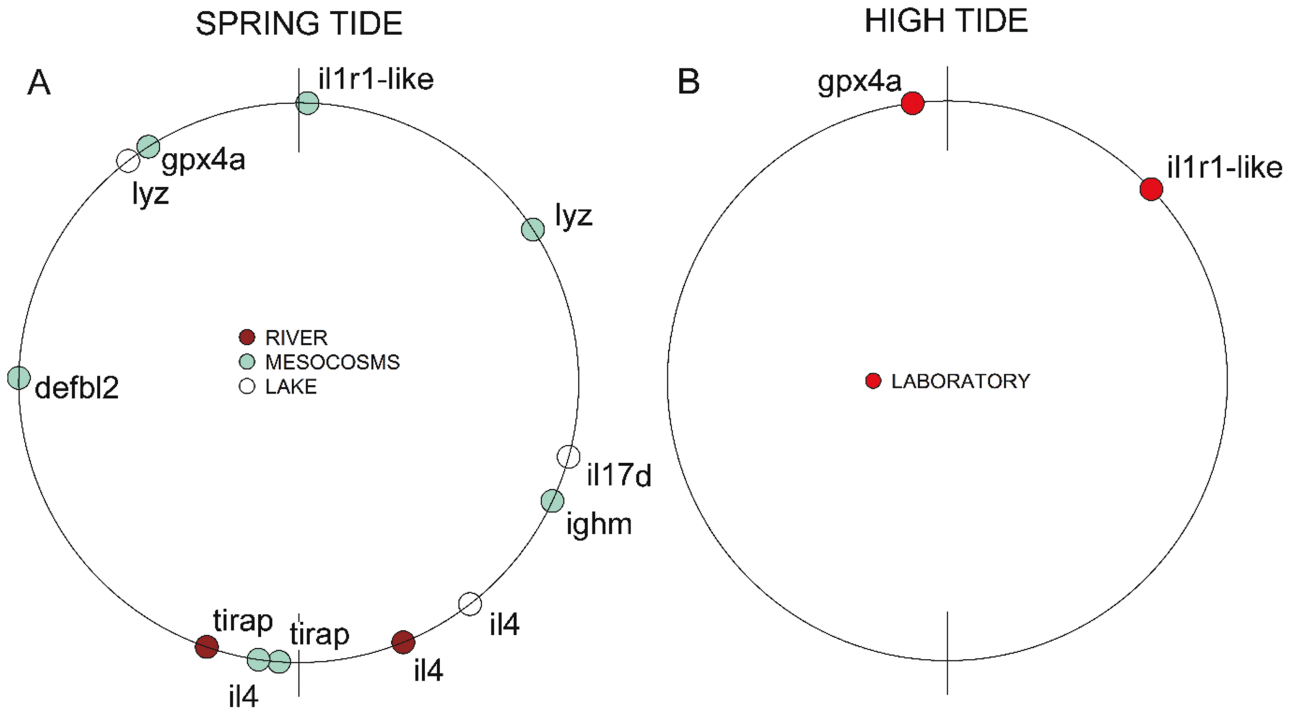

Figure 6: timing of individually significant gene expression cycles where there was overall significance in a given habitat. Clockwise circular plots showing the acrophase of gene expression maxima in radians zeroed on the acrophase for the corresponding physical cycle (the highest amplitude spring tide for semicircalunar cycles and high tide for tidal cycles). (A) semicircalunar cycles at field sites. (B) Circatidal cycles in the laboratory

Table 1: significant circatidal cycles in the expression of individual genes in the laboratory population. Results from LMMs showing: the test statistic, degrees of freedom, and *P* value for a likelihood ratio test; the reduction in Akaike Information Criterion when the sinusoid terms were added to a base model (for models fitted by Maximum Likelihood); β and *γ* coefficients for the sinusoid terms [38]; and the acrophase (Φ, radians) zeroed on the local tidal height acrophase

Gene	X^2	*DF*	*P*	ΔAIC	*β*	*γ*	$\Phi^{\text{tidal zero}}$
Il1r1-like	6.41	2	0.040	2.4	−0.05 ± 0.11	0.23 ± 0.09	0.82
gpx4a	6.10	2	0.047	2.1	−0.30 ± 0.13	0.06 ± 0.11	−0.12

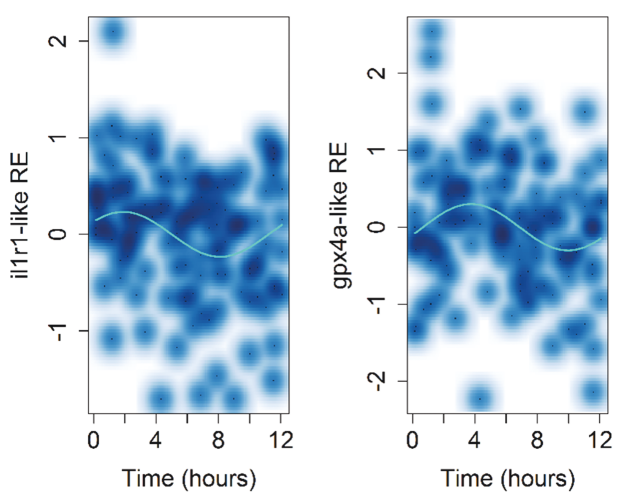

Figure 7: smoothed density scatterplot of gene relative expression (RE) partial residuals against time (decimal tidal phase point) with line showing the predicted tidal sinusoid from an LMM. (A) RE for *il1r1*-like. (B) RE for *gpx4a*

These observations are consistent with an endogenous tidal rhythm as the laboratory population lacked obvious tidal environmental cues and the sampling regimen employed avoided significant collinearity amongst predictors of the different relevant circannual and lunar cycles. In contrast, we could not detect circatidal rhythmicity in overall tests in wild and mesocosm populations of sticklebacks (exposed to natural lighting and weather). However, in the case of these field localities, it is important to note that our ability to detect circatidal rhythms may have been limited by collinearity in circannual and lunar cycles under the monthly sampling regimen adopted. Furthermore, the low amplitude modality seen in the laboratory environment may have been suppressed or masked by environmental variability in the wild.

We found no evidence of circasemilunar or circalunar oscillations in the laboratory fish, suggesting a lack of any endogenous rhythms with these periodicities. On the other hand, we consistently detected small circasemilunar modalities in the wild populations, which had overall significance and affected several genes. This may indicate that the circasemilunar patterns in the field were driven by environmental cues. It is

also possible that, due to collinearity in the monthly field sampling regimen, semicircalunar cycles might have been poorly distinguishable from tidal cycles or circannual cycles, especially if the latter (which were substantial) were complex and not fully described by a simple sinusoid pattern.

The small lunar modalities that we observed occurred against the expected dominant background of circannual oscillation that we have previously reported [11]. Although we took a somewhat different approach to data transformation and analysis here than previously, we nonetheless still found dominant, high amplitude circannual cycling in outdoors populations. We have previously demonstrated that these cycles are driven by a combination of environmental temperature and seasonal diet changes and not by photoperiodic seasonal control, by an endogenous seasonal cycle, or by an intersection with a circadian cycle [11, 37]. As previously described, in these wild circannual cycles two distinctive sets of genes consistently vary in approximate anti-phase, with expression maxima in one set tending towards late summer and the other set towards late winter. Also as previously described, we found a circannual rhythm in laboratory sticklebacks that was much smaller and very distinct to the wild circannual oscillations, although considerably larger than the small laboratory tidal rhythm described above. We have previously tentatively inferred that the circannual rhythm in laboratory sticklebacks is a non-photoperiodically entrained endogenous rhythm as it occurs independent of manipulations of seasonal photoperiod. It is fundamentally distinct to the large amplitude winter–summer oscillation seen in field populations, predominantly with spring expression maxima 90° out-of-phase with the environmentally driven circannual cycles in the wild [11]. The present study confirms that the large field circannual oscillations could not be due to endogenous lunar cycles as these are either absent in laboratory fish or of much smaller magnitude than the field oscillation.

Although we detected only a very small tidal modality, our data support the possibility of a tidal clock that can persist outside of the immediate marine environment in vertebrate animals. Recently, robust expression modalities inconsistent with a circadian rhythm, with 8-hour and 12-hour periods and affecting thousands of genes, including important immunological genes, have been demonstrated in mice [7]. In the case of the 12-hour rhythm, this coincides with elevated dawn and dusk activity and has been shown to be transcriptionally regulated by Spliced Form of X-box Binding Protein 1 (XBP1s). This non-circadian clock may have evolved from a tidal clock as XBP1s and conserved sets of transcripts cycling detectably with a 12-hour period are present in primitive marine organisms such as Cnidaria [5]. Thus, if the 12-hour dawn–dusk clock in mice has evolved from a tidal cycle, we might expect to see evidence of an unmodified c. 12-hour tidal cycle in recently marine-derived vertebrates. This is what we have found in the present study.

In the laboratory population, the only two individually significant genes with tidal modalities were *gpx4a*, which is a major antioxidant gene in fish [47], protecting cells against oxidative damage, and *il1rl*, which is a member of the interleukin 1 receptor family and involved in innate immune signaling pathways [25]. The acrophase for both of these genes was consistent with highest expression near high tide on the local coastline. Speculatively, this could indicate an adaptive readiness for higher innate immune reactivity and protection from the oxidative stress that might result from this [16], due to behavioral changes or environmental changes across the tidal cycle. Interestingly, moreover, *gpx4a* and *il1rl* featured amongst the apparent circasemilunar cycling genes in the wild populations, where their expression maxima were close to the high tidal amplitude (spring tide) point of the tidal cycles on the local coastline. Notwithstanding, these and other genes with detectable apparent circasemilunar cycling in the wild populations also tended to be genes with winter circannual expression maxima when peaking in the spring (high amplitude) half of the circasemilunar cycle and to be genes with summer circannual expression maxima when peaking in the neap (low amplitude) half of the cycle. These coincidences of timing may reflect the possibility, discussed above, that the observed circasemilunar modalities in wild populations may originate from collinear circannual or tidal modalities.

In summary, in the present study, we have found that ultradian circatidal cycles in immune expression can be conserved in vertebrates even where these have evolved to exploit habitats outside of the immediate marine environment. This is consistent with the existence of a primordial tidal clock affecting the immune system, and with previous suggestions that such a clock could drive biological rhythms that are separate from the well-known circadian clock in other non-marine vertebrates. This may have practical implications. For example, in finfish aquaculture additional research might be warranted in relation to the effect of tidal cycles on vaccination efficacy or disease susceptibility, particularly in organisms with marine-linked life histories. In general, the possibility of biological rhythms in the immune system other than circadian rhythms should be given more attention.

Acknowledgements

We are very grateful to many colleagues who have contributed to our previous studies on three-spined sticklebacks and who were included as coauthors of, or mentioned in the acknowledgements of, those studies. The Editor-in-Chief, Simon Milling, and handling editor, Kathryn Else, would like to thank the two anonymous reviewers for their contribution to the publication of this article.

Ethical approval

The animal studies generating the datasets employed in the present study have fully followed institutional and national ethical regulations and guidelines. Work involving regulated scientific procedures as defined in the Animal (Scientific Procedures) Act 1987 (ASPA) was conducted under UK Home Office (HO) License PPL 302876 held at Cardiff University and all other work was designed in consultation with the ASPA HO inspectorate.

Conflicts of interest

None declared.

Funding

This work was supported by Leverhulme Trust Research grant RPG-301.

Data availability

This study is based on previously described datasets that will be available in the European Nucleotide Archive (primary accession number PRJEB13319).

Author contributions

This manuscript is based on previously described datasets. J.A.J. analyzed the data. J.A.J., J.C., and A.S. wrote the manuscript.

References

1. Man K, Loudon A, Chawla A. Immunity around the clock. Science 2016, **354**, 999–1003. doi:10.1126/science.aah4966
2. Andreatta G, Tessmar-Raible K. The still dark side of the moon: molecular mechanisms of lunar-controlled rhythms and clocks. J Mol Biol 2020, **432**, 3525–46. doi:10.1016/j.jmb.2020.03.009
3. Tessmar-Raible K, Raible F, Arboleda E. Another place, another timer: marine species and the rhythms of life. Bioessays 2011, **33**, 165–72. doi:10.1002/bies.201000096
4. Kaiser TS, Neumann J. Circalunar clocks—old experiments for a new era. Bioessays 2021, **43**, 2100074.
5. Pan Y, Ballance H, Meng H, Gonzalez N, Kim SM, Abdurehman L, et al. 12-h clock regulation of genetic information flow by XBP1s. PLoS Biol 2020, **18**, e3000580. doi:10.1371/journal.pbio.3000580
6. Ballance H, Zhu B. Revealing the hidden reality of the mammalian 12-h ultradian rhythms. Cell Mol Life Sci 2021, **78**, 3127–40. doi:10.1007/s00018-020-03730-5
7. Zhu B, Zhang Q, Pan Y, Mace EM, York B, Antoulas AC, et al. A cell-autonomous mammalian 12 hr clock coordinates metabolic and stress rhythms. Cell Metab 2017, **25**, 1305–19.e9. doi:10.1016/j.cmet.2017.05.004
8. Cermakian N, Stegeman SK, Tekade K, Labrecque N. Circadian rhythms in adaptive immunity and vaccination. Semin Immunopathol 2022, **44**, 193–207. doi:10.1007/s00281-021-00903-7
9. Palomino-Segura M, Hidalgo A. Circadian immune circuits. J Exp Med 2020, **218**, e20200798.
10. Spence R, Wootton RJ, Barber I, Przybylski M, Smith C. Ecological causes of morphological evolution in the three-spined stickleback. Ecol Evol 2013, **3**, 1717–26. doi:10.1002/ece3.581
11. Stewart A, Hablützel PI, Watson HV, Brown M, Friberg IM, Cable J, et al. Physical cues controlling seasonal immune allocation in a natural piscine model. Front Immunol 2018, **9**, 582. doi:10.3389/fimmu.2018.00582
12. Stewart A, Hablützel PI, Brown M, Watson HV, Parker-Norman S, Tober AV, et al. Half the story: thermal effects on within-host infectious disease progression in a warming climate. Global Change Biol 2018, **24**, 371–86. doi:10.1111/gcb.13842
13. Reid K, Bell MA, Veeramah KR. Threespine stickleback: a model system for evolutionary genomics. Annu Rev Genomics Hum Genet 2021, **22**, 357–83. doi:10.1146/annurev-genom-111720-081402
14. Wootton RJ, Smith C. A Long-term study of a short-lived fish: the demography of *Gasterosteus aculeatus*. Behaviour 2000, **137**, 981–97.
15. Prugh LR, Golden CD. Does moonlight increase predation risk? Meta-analysis reveals divergent responses of nocturnal mammals to lunar cycles. J Anim Ecol 2014, **83**, 504–14. doi:10.1111/1365-2656.12148
16. Hablützel PI, Brown M, Friberg IM, Jackson JA. Changing expression of vertebrate immunity genes in an anthropogenic environment: a controlled experiment. BMC Evol Biol 2016, **16**, 175. doi:10.1186/s12862-016-0751-8
17. Zou J, Mercier C, Koussounadis A, Secombes C. Discovery of multiple beta-defensin like homologues in teleost fish. Mol Immunol 2007, **44**, 638–47. doi:10.1016/j.molimm.2006.01.012
18. Nakanishi T, Toda H, Shibasaki Y, Somamoto T. Cytotoxic T cells in teleost fish. Dev Comp Immunol 2011, **35**, 1317–23. doi:10.1016/j.dci.2011.03.033
19. Zhang Q, Geng M, Li K, Gao H, Jiao X, Ai K, et al. TGFβ1 suppresses the T-cell response in teleost fish by initiating Smad3- and Foxp3-mediated transcriptional networks. J Biol Chem 2023, **299**, 102843. doi:10.1016/j.jbc.2022.102843
20. Bain PA, Schuller KA. A glutathione peroxidase 4 (GPx4) homologue from southern bluefin tuna is a secreted protein: first report of a secreted GPx4 isoform in vertebrates. Comp Biochem Physiol B Biochem Mol Biol 2012, **161**, 392–7. doi:10.1016/j.cbpb.2012.01.004
21. Bilal S, Etayo A, Hordvik I. Immunoglobulins in teleosts. Immunogenetics 2021, **73**, 65–77. doi:10.1007/s00251-020-01195-1
22. Gambón-Deza F, Sánchez-Espinel C, Magadán-Mompó S. Presence of an unique IgT on the IGH locus in three-spined stickleback fish (*Gasterosteus aculeatus*) and the very recent generation of a repertoire of VH genes. Dev Comp Immunol 2010, **34**, 114–22. doi:10.1016/j.dci.2009.08.011
23. Wang X, Zhang A, Qiu X, Yang K, Zhou H. The IL-12 family cytokines in fish: molecular structure, expression profile and function. Dev Comp Immunol 2023, **141**, 104643. doi:10.1016/j.dci.2023.104643
24. Liu X, Sun S, Liu D. IL-17D: a less studied cytokine of IL-17 family. Int Arch Allergy Immunol 2020, **181**, 618–23. doi:10.1159/000508255
25. Sebo DJ, Fetsko AR, Phipps KK, Taylor MR. Functional identification of the zebrafish Interleukin-1 receptor in an embryonic model of Il-1β-induced systemic inflammation. Front Immunol 2022, **13**, 1039161. doi:10.3389/fimmu.2022.1039161
26. Ohtani M, Hayashi N, Hashimoto K, Nakanishi T, Dijkstra JM. Comprehensive clarification of two paralogous interleukin 4/13 loci in teleost fish. Immunogenetics 2008, **60**, 383–97. doi:10.1007/s00251-008-0299-x
27. Tian H, Xing J, Tang X, Sheng X, Chi H, Zhan W. Cytokine networks provide sufficient evidence for the differentiation of CD4+ T cells in teleost fish. Dev Comp Immunol 2023, **141**, 104627. doi:10.1016/j.dci.2022.104627
28. Li L, Cardoso JCR, Félix RC, Mateus AP, Canário AVM, Power DM. Fish lysozyme gene family evolution and divergent function in early development. Dev Comp Immunol 2021, **114**, 103772. doi:10.1016/j.dci.2020.103772
29. Vaeth M, Kahlfuss S, Feske S. CRAC channels and calcium signaling in T cell-mediated immunity. Trends Immunol 2020, **41**, 878–901. doi:10.1016/j.it.2020.06.012
30. Clément J-F, Meloche S, Servant MJ. The IKK-related kinases: from innate immunity to oncogenesis. Cell Res 2008, **18**, 889–99. doi:10.1038/cr.2008.273
31. Purcell MK, Smith KD, Aderem A, Hood L, Winton JR, Roach JC. Conservation of Toll-like receptor signaling pathways in teleost fish. Comp Biochem Physiol D Genomics Proteomics 2006, **1**, 77–88. doi:10.1016/j.cbd.2005.07.003
32. Livak KJ, Schmittgen TD. Analysis of relative gene expression data using real-time quantitative PCR and the 2(-Delta Delta C(T)) Method. Methods 2001, **25**, 402–8. doi:10.1006/meth.2001.1262
33. Brown M, Hablützel P, Friberg IM, Thomason AG, Stewart A, Pachebat JA, et al. Seasonal immunoregulation in a naturally-occurring vertebrate. BMC Genomics 2016, **17**, 369. doi:10.1186/s12864-016-2701-7
34. Forsythe WC, Rykiel EJ, Stahl RS, Wu H-i, Schoolfield RM. A model comparison for daylength as a function of latitude and day of year. Ecol Model 1995, **80**, 87–95. doi:10.1016/0304-3800(94)00034-f
35. Hijmans RJ. geosphere: Spherical Trigonometry, 2022. R package version 1.5-18. https://CRAN.R-project.org/package=geosphere (1 October 2023, date last accessed).

36. Astronomical Applications Department of the U.S. Naval Observatory, 2023. https://aa.usno.navy.mil/index (1 October 2023, date last accessed).
37. Jackson JA, Friberg IM, Hablützel PI, Masud N, Stewart A, Synnott R, et al. Partitioning the environmental drivers of immunocompetence. Sci Total Environ 2020, **747**, 141152. doi:10.1016/j.scitotenv.2020.141152
38. Cornelissen G. Cosinor-based rhythmometry. Theor Biol Med Model 2014, **11**, 16. doi:10.1186/1742-4682-11-16
39. Halberg F. Chronobiology. Annu Rev Physiol 1969, **31**, 675–725. doi:10.1146/annurev.ph.31.030169.003331
40. R Core Team. *R: A Language and Environment for Statistical Computing*. Vienna: R Foundation for Statistical Computing, 2023.
41. Peterson RA, Cavanaugh JE. Ordered quantile normalization: a semiparametric transformation built for the cross-validation era. J Appl Statist 2020, **47**, 2312–27. doi:10.1080/02664763.2019.1630372
42. Hadfield JD. MCMC methods for multi-response generalized linear mixed models: the MCMCglmm R package. J Stat Software 2010, **33**, 1–22.
43. Bates D, Mächler M, Bolker B, Walker S. Fitting linear mixed-effects models using lme4. J Stat Software 2015, **67**, 1 –48.
44. Fisher RA. *Statistical Methods for Research Workers*. Edinburgh: Oliver & Boyd, 1925.
45. Bingham C, Arbogast B, Guillaume GC, Lee JK, Halberg F. Inferential statistical methods for estimating and comparing cosinor parameters. Chronobiologia 1982, **9**, 397–439.
46. Hoffman GE, Schadt EE. variancePartition: interpreting drivers of variation in complex gene expression studies. BMC Bioinf 2016, **17**, 483. doi:10.1186/s12859-016-1323-z
47. Grim JM, Hyndman KA, Kriska T, Girotti AW, Crockett EL. Relationship between oxidizable fatty acid content and level of antioxidant glutathione peroxidases in marine fish. J Exp Biol 2011, **214**, 3751–9. doi:10.1242/jeb.058214